ARTICLE

OBC
www.rsc.org/obc

Protonated canthaxanthins as models for blue carotenoproteins† ‡

Geir Kildahl-Andersen, Bjart Frode Lutnaes and Synnøve Liaaen-Jensen*
Department of Chemistry, Norwegian University of Science and Technology (NTNU), NO-7491 Trondheim, Norway. E-mail: slje@chem.ntnu.no; Fax: +47 73594256; Tel: +47 73594099

Received 15th October 2003, Accepted 4th December 2003
First published as an Advance Article on the web 21st January 2004

It has been suggested that astaxanthin (3,3′-dihydroxy-β,β-carotene-4,4′-dione) in the carotenoprotein α-crustacyanin occurs in the diprotonated form. As a model system for protonated astaxanthin in α-crustacyanin the reactions of canthaxanthin (β,β-carotene-4,4′-dione) with Brønsted acids (CF_3COOH and CF_3SO_3H) and the Lewis acid BF_3–etherate have been investigated. Structures of C-5 protonated, C-7 protonated, enolised O-4 protonated and O-4,4′, C-7 triprotonated canthaxanthin have been established by VIS-NIR and NMR spectroscopy. The charge distribution in the cations has been considered by comparison of the ^{13}C chemical shift difference relative to neutral relevant carotenoid models. The experimental evidence for protonated canthaxanthins differs significantly from previous AM1 calculations. Experimental data for O-4,4′, C-7 triprotonated canthaxanthin relative to C-7 protonated canthaxanthin is considered a relevant model for O-4,4′ diprotonated canthaxanthin, in comparison with neutral canthaxanthin. The positive charge was mainly located at C-6/6′ ⩾ C-8/8′ > C-10/10′ > C-12/12′ > C-14/14′ ~ C-15/15′ in the polyene chain. Moreover, it was inferred that only 14% of the positive charge is delocalised to the polyene chain, the remaining charge must therefore be located at the protonated carbonyl moiety. The results are discussed in relation to previous solid state NMR studies of ^{13}C labelled astaxanthin in α-crustacyanin and recent X-ray analysis of β-crustacyanin.

Introduction

Conjugated keto-carotenoids, usually astaxanthin (**1**), are complexed stoichiometrically with the protein in true carotenoproteins. Such carotenoproteins are usually purple–blue and are encountered particularly in the carapace of *Crustaceaea* and in the skin of *Echinodermata*.[1] Our group has been involved in earlier studies on crustacyanin,[2] asteriarubin,[3] alloporin[4] and linckiacyanin.[5] The VIS absorption spectra of these carotenoproteins are compiled in Fig. 1. Crustacyanin from lobster carapace is the best studied carotenoprotein.[1,6–9]

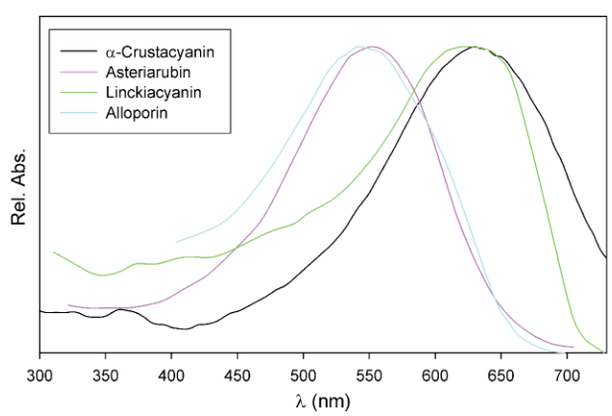

Fig. 1 VIS spectra of carotenoproteins in aqueous buffer solution.[2–5]

Astaxanthin (**1**) is not covalently bound in carotenoproteins and is released by solvent (acetone) extraction. A colourless apoprotein is thereby obtained. The blue colour may be reconstituted by recombination of the apoprotein with a range of conjugated keto-carotenoids.[3,4,10,11]

The colour shift from red (**1**, λ_{max} 472 nm in hexane) to blue (crustacyanin, λ_{max} 632 nm in phosphate buffer) is among the largest shifts recorded in Nature and has received much attention.[7–9,12–15]

In the early nineties we established the chemistry behind the classical colour test of epoxidic carotenoids which are providing a blue colour when treated with strong acids. The blue products were identified as oxonium ions.[16] In our mind this finding offered a clue to the understanding of the bathochromic shift of astaxanthin (**1**) when bound to carotenoproteins. Indeed, recent results have suggested a polarisation of the chromophore in crustacyanin, compatible with protonation of the keto groups in **1**,[17] providing carboxonium ions. These studies were further pursued, using modern physical methods including solid-state NMR and resonance Raman.[8,17,18] At a time acidic amino acids were suggested to be responsible for the protonation of the keto groups.[12]

Refined X-ray data for β-crustacyanin[7] have recently identified the contacts between astaxanthin (**1**) and the protein surroundings. α-Crustacyanin consists of eight β-crustacyanin (λ_{max} 585 nm) units, each containing two astaxanthin molecules in different surroundings.[6,7]

In this work we aimed at preparing protonated, positively charged species of canthaxanthin (**2**), with the di-*O*-protonated dication **3** as target molecule, Scheme 1, to be characterised by NIR and NMR spectroscopy, as a model for the carotenoids of blue carotenoproteins.

We have recently successfully prepared from β,β-carotene (**4**), and characterised by NIR, ^1H and ^{13}C NMR spectroscopy, the dication **5** obtained by reaction with BF_3–etherate,[19,20] and from isocryptoxanthin (**6**, β,β-caroten-4-ol) the monocations **7** and **8**, obtained by treatment with CF_3COOH,[21] Scheme 2. Dotted bonds demonstrate regions of bond inversion, and the diameter of the filled circles illustrates the distribution of the positive charge in the carbocations studied. Similar techniques were considered for the characterisation of protonated canthaxanthin (**3**).

† Electronic supplementary information (ESI) available: ^1H and 2D ROESY NMR spectra of **9/10** and **14** and ^1H NMR spectrum of **9/10/12/13** in CD_2Cl_2 at −15 °C. See http://www.rsc.org/suppdata/ob/b3/b313639f/

‡ Part 4 in the series: Charged carotenoids species. For part 3 see ref. 20.

DOI: 10.1039/b313639f

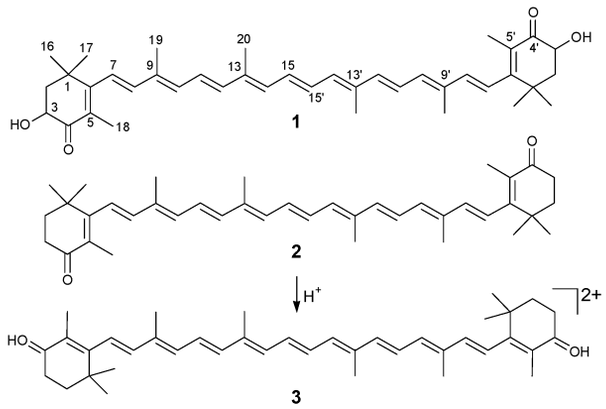

Scheme 1

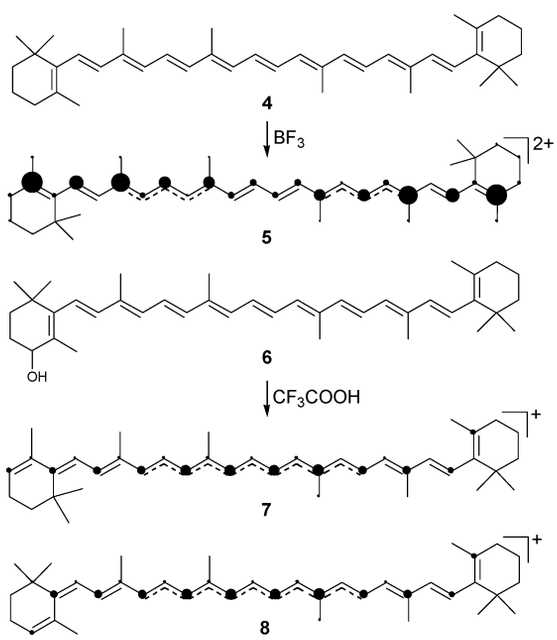

Scheme 2

Results

Treatment of canthaxanthin (2) with CF_3COOH

Synthetic canthaxanthin (**2**) in CH_2Cl_2 solution was treated with CF_3COOH in various concentrations at −15 °C. With dilute acid a λ_{max} of 503 nm was observed, with a weak absorption at 881 nm, Fig. 2. Higher concentration of acid gave increased absorption at the longer wavelength. At 1 M concentration of CF_3COOH a stable λ_{max} of 871 nm was observed, consistent with previous observations.[22]

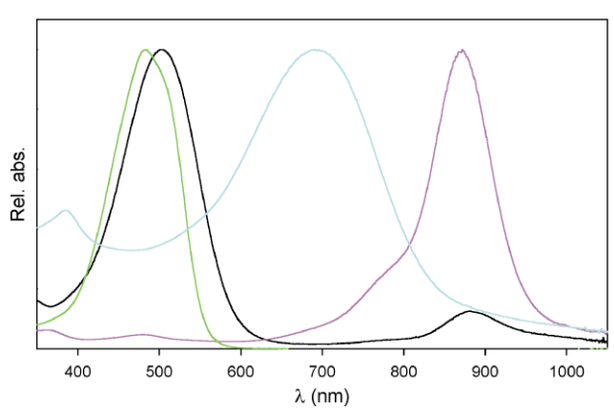

Fig. 2 VIS/NIR spectra of canthaxanthin (**2**) (green), with 13 mM CF_3COOH (black), with 1 M CF_3COOH (magenta), and with 11 mM CF_3SO_3H (cyan), all in CH_2Cl_2 at −15 °C.

^{1}H, ^{1}H–^{1}H COSY, 2D ROESY, ^{1}H–^{13}C HSQC, ^{1}H–^{13}C HMBC and 2D *J*-resolved ^{1}H NMR spectra were recorded of the product prepared *in situ* at −15 °C using CF_3COOD (Sigma). The NMR data revealed the presence of monocations of canthaxanthin deuteronated in the 7-position (**9**) and in the 5-position (**10**) in a 2 : 3 ratio. In the following, the deuteronated products prepared by reaction with deuterated acids for NMR studies are referred to as protonated.

^{1}H and ^{13}C chemical shifts and $^3J_{H,H}$, $^1J_{C,H}$ and long-range coupling constants for products **9** and **10** are given in Table 1. For the C-7 protonated product **9**, long-range coupling was observed from Me-19 to H-8, from Me-19′ to H-10′ and from Me-20′ to H-14′. From the coupling constants between H-10 and H-11 it may be inferred that the C-10,11 bond is a double bond.[19–21] Bond inversion is therefore allocated to the C-12 to C-15′ region.

The long-range couplings observed for **9** were also observed for the C-5 protonated product **10**. The observed coupling constants between H-10 and H-11 and H-11 and H-12 are very similar, and of an intermediate size (*ca*. 13 Hz). Hence the region for bond inversion was therefore assigned to the C-10 to C-15′ region for **10**.

The stereochemistry of the C-6,7 bond in **10** followed from cross-peaks in the 2D ROESY spectrum between Me-16/17 and H-7 and between Me-18 and H-8. The isomer with rotated end groups, *cf*. ref. 19–21 was not observed.

The charge distribution in the charged carotenoids **9** and **10** may in principle be determined by the ^{13}C chemical shift differences for each atom in the charged molecules relative to the corresponding uncharged molecule.[19–21,23] Exact determination of the distribution of the positive charge in **9** and **10** is problematic due to the lack of ideal neutral model carotenoids. However, ^{1}H and ^{13}C chemical shifts are published for the carotenoid end group **11**,[24] here used as a model for C-1 to C-11 and C-16/17/18/19 in comparison with the C-7 protonated **9**. For the remaining positions, canthaxanthin (**2**) was used as the neutral model (**11**/**2**), Scheme 3.

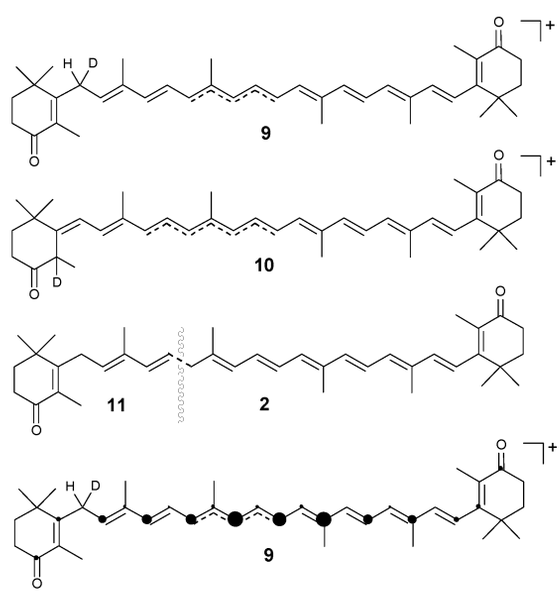

Scheme 3

The ^{13}C shift differences resulting from the comparison of the C-7 protonated canthaxanthin (**9**) with the relevant neutral model are compiled in Table 2. Highest positive charge (largest shift differences) appears to be in the central region at C-14, C-15′ and C-13′ for **9**, illustrated at the bottom of Scheme 3. The total ^{13}C shift difference for all carbon atoms in **9**, $\Sigma\Delta\delta_C$ = 260 ppm is consistent with one positive charge.[19–21,23]

Table 1 ^{1}H and ^{13}C chemical shifts, $^{3}J_{H,H}$ and $^{1}J_{C,H}$ coupling constants and long-range couplings for C-7 and C-5 protonated canthaxanthin (**9** and **10**)

	C-7 protonated canthaxanthin (**9**)				C-5 protonated canthaxanthin (**10**)			
	δ_C (ppm)	δ_H (ppm)	$^{3}J_{H,H}$/Hz	$^{1}J_{C,H}$/Hz	δ_C (ppm)	δ_H (ppm)	$^{3}J_{H,H}$/Hz	$^{1}J_{C,H}$/Hz
1	36.5				37.3			
2	36.0	1.89			33.8	1.82/2.10		
3	33.0	2.66			35.0	2.61/2.80		
4	206.3				223.1			
5	132.1				47.1			
6	171.2				163.6			
7	31.8	3.35	6.6		122.1	6.69	12.9	150
8	145.9	6.00	6.6		144.3	7.05	12.9	
9	139.0				139.8			
10	158.6	7.17	14.8		162.6	7.43	13.6	
11	126.0	6.94			127.8	7.09	13.2/13.6	
12	162.6	7.41			164.4	7.53	13.2	
13	142.8				143.0			
14	168.8	7.72			167.0	7.67	13.3	
15	133.3	7.16			133.3	7.15	13.1/13.3	
16	25.8	1.17		127	28.8	1.25		127
17	25.8	1.17		127	29.8	1.35		127
18	11.4	1.72		127	21.6	1.46		131
19	12.5	2.04	H-8[a]	128	12.4	2.12	H-8[a]	127
20	12.6	2.18			12.6	2.20	H-12[a]	
1′	36.8				36.8			
2′	36.0	1.91		130	36.0	1.91		130
3′	33.0	2.71		130	33.0	2.71		130
4′	206.5				206.5			
5′	130.4				130.4			
6′	168.8				169.9			
7′	132.8	6.82	16.1		130.7	6.72	16.4	
8′	142.1	6.57	16.1		142.7	6.56	16.4	
9′	152.5				148.7			
10′	136.3	6.68	11.5		136.3	6.62	11.3	
11′	145.0	7.86	11.5/15.1		141.0	7.65	11.3/14.9	
12′	139.8	6.92	15.1		139.8	6.84	14.9	
13′	170.8				165.3			
14′	138.4	7.02			137.9	6.93	13.1	
15′	161.2	8.10			158.0	7.97	13.1/13.1	
16′/17′	27.0	1.22		127	27.0	1.22		127
18′	13.8	1.89		129	13.8	1.90		129
19′	13.7	2.27	H-10′[a]	128	13.3	2.22	H-10′[a]	128
20′	15.0	2.48	H-14′[a]	129	14.5	2.41	H-14′[a]	129

[a] Indicates long-range coupling from methyl groups.

Table 2 ^{13}C chemical shifts (ppm) of model compound (**11/2**), and calculated chemical shift difference between C-7 protonated canthaxanthin (**9**) and the model compound

Carbon	δ_C, Model	$\Delta\delta_c$, **9**	Carbon	δ_C, Model	$\Delta\delta_c$, **9**
1	36.4	0.1	1′	35.7	1.1
2	37.4	−1.4	2′	37.7	−1.7
3	34.3	−1.3	3′	34.3	−1.3
4	198.9	7.4	4′	198.7	7.8
5	131.6	0.5	5′	129.9	0.5
6	163.2	8.0	6′	160.9	7.9
7	30.1	1.7	7′	124.2	8.6
8	129.8	16.1	8′	141.1	1.0
9	135.5	3.5	9′	134.8	17.7
10	137.4	21.2	10′	134.2	2.1
11	123.7	2.3	11′	124.7	20.3
12	139.3	23.3	12′	139.3	0.5
13	136.6	6.2	13′	136.6	34.2
14	133.6	35.2	14′	133.6	4.8
15	130.5	2.8	15′	130.5	30.7
16/17	26.7	−0.9	16′/17′	27.7	−0.7
18	11.4	0.0	18′	13.7	0.1
19	12.8	−0.3	19′	12.5	1.2
20	12.7	−0.1	20′	12.7	2.3
				$\Sigma\Delta\delta_C$	259.8

Treatment of canthaxanthin (**2**) in CD_2Cl_2 with CF_3COOD from another manufacturer (Acros) gave a different and more complex product mixture of protonated canthaxanthins in reproducible experiments. Besides the C-7 protonated (**9**) and C-5 protonated (**10**) products characterised above, were two additional and major monocations **12** and **13**, in a ratio 2 : 1 : 4 : 3 respectively, identified by NMR analysis. ^{1}H and ^{13}C chemical shift data for products **12** and **13**, and $^{3}J_{H,H}$, $^{1}J_{C,H}$ and long-range couplings for **12** are given in Table 3. These additional products (**12** and **13**) differed in the stereochemistry of the C-6,7 double bond.

In contrast to the C-7 protonated (**9**) and C-5 protonated (**10**) products, the polyene chain had unbroken conjugation. The C-16 and C-17 methyl groups were identical, as were the two geminal protons at C-2 and at C-3, suggesting that C-4 was still sp^2-hybridised. However, the ^{13}C chemical shift for C-4 was only 150 ppm, incompatible with carbonyl. The plausible formation of **12** and **13**, shown in Scheme 4, is considered in the Discussion.

The determination of the charge distribution in **12** and **13** also suffers from the lack of relevant carotenoid models. Some information is gained, however, by comparison of the charged products **9**, **10** and **12** with neutral canthaxanthin (**2**). The four protonated canthaxanthins **9**, **10**, **12** and **13** may all be represented by resonance structures with positive charges at the carbon atoms considered in Fig. 3.

Similar distribution of the charge towards the centre of the polyene chain available for charge delocalisation is demonstrated for all the three monocations **9**, **10** and **12**. For **9** and **10**, the polyene chain has been shortened by the proton added at

Table 3 ^{1}H and ^{13}C chemical shifts (ppm), $^{3}J_{H,H}$ and $^{1}J_{C,H}$ coupling constants (Hz) for the enolic O-4 protonated canthaxanthins **12** and **13**

	12			**13**		
	δ_C	δ_H	$^{3}J_{H,H}$	$^{1}J_{C,H}$	δ_C	δ_H
1	37.7				38.8	
2	35.1	1.75			36.1	1.77
3	24.8	2.50			24.8	2.51
4	151.1				152.7	
5	123.5				125.8	
6	162.9				160.9	
7	122.3	6.69	13.1	152	123.5	6.74
8	150.7	7.37			150.7	7.75
9	140.5					
10	163.8	7.46	13.8	155		
11	128.0	7.12		159		
12	164.8	7.52		154		
13	142.9					
14	165.3	7.60	13.1	155		
15	133.3	7.13		156		
16/17	26.8	1.23		127	29.0	1.43
18	17.5	2.00	H-3[a]	130	12.1	1.88
19	11.8	2.13	H-8[a]	128		
20	12.4	2.19		128		
1′	36.7					
2′	35.8	1.90		130		
3′	32.8	2.71		130		
4′	206.5					
5′	130.1					
6′	170.9					
7′	129.6	6.66	14.3	159		
8′	142.7	6.56		159		
9′	146.6					
10′	136.2	6.59		154		
11′	138.9	7.54				
12′	139.7	6.79	14.5	154		
13′	162.1					
14′	137.2	6.87	13.0	156		
15′	156.1	7.87				
16′/17′	26.8	1.22		127		
18′	13.6	1.90	H-7′[a]	128		
19′	12.4	2.18	H-10′[a]			
20′	14.1	2.36	H-14′[a]	128		

[a] Indicates long-range coupling from methyl groups.

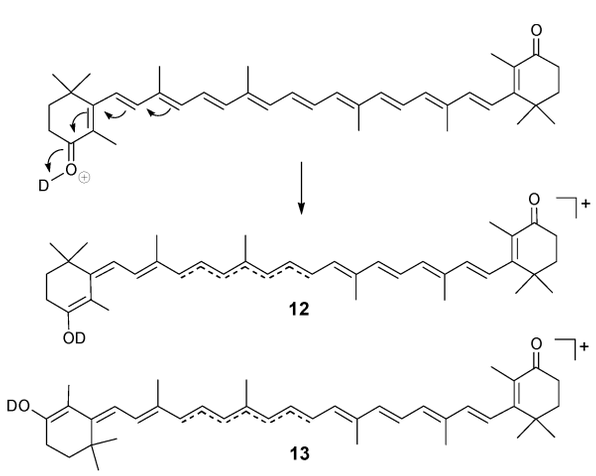

Scheme 4

the left side of the structure, Scheme 3, forcing the centre of the charge more towards the right in the polyene chain, Fig. 3.

The positive charge of these monocations (**9**, **10**, **12**) may be distributed over 19, 21 and 23 carbons atoms, respectively. As may be seen from Fig. 3, a shorter polyene chain also leads to a higher partial charge at each carbon.

Hydrolysis of protonated canthaxanthins, prepared with CF_3COOH, provided strongly *cis*-isomerised canthaxanthin (**2**), compatible with the capture of a proton from the cations by

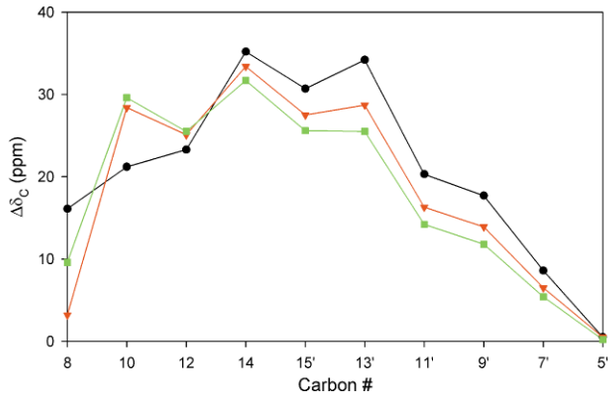

Fig. 3 ^{13}C chemical shift differences $\Delta\delta_C$ for selected downfield shifted carbon atoms of C-7 protonated canthaxanthin (**9**) − model (**11/2**) (black), C-5 protonated canthaxanthin (**10**) − **2** (red) and for O-4 protonated and enolised canthaxanthin (**12**) − **2** (green).

water. *Cis–trans* isomerisation of carotenoids readily occurs *via* cationic intermediates.[20,21,25]

Assignments of NMR spectra of the pink product (λ_{max} 503 nm), formed by treatment of canthaxanthin (**2**) with dilute CF_3COOD, failed because of signal broadening. Even when the temperature was lowered to −70 °C, only the geminal methyl groups (H-16/17/16′/17′) and methylene protons (H-2/3/2′/3′) could be seen as relatively sharp peaks.

Treatment of canthaxanthin (2) with CF_3SO_3H

A weaker Brønsted acid than CF_3COOH (CH_3COOH) gave no protonation of canthaxanthin (**2**). Use of the stronger acid CF_3SO_3H caused immediate protonation with NIR absorption around 692 nm, Fig. 2.

Product analysis by NMR, as described above, led to the identification of the trication **14**, protonated at O-4, O-4′ and C-7, Scheme 5, including in-space interactions from ROESY data. ^{1}H and ^{13}C chemical shifts and $^{1}J_{C,H}$ and $^{3}J_{H,H}$ coupling constants are given in Table 4.

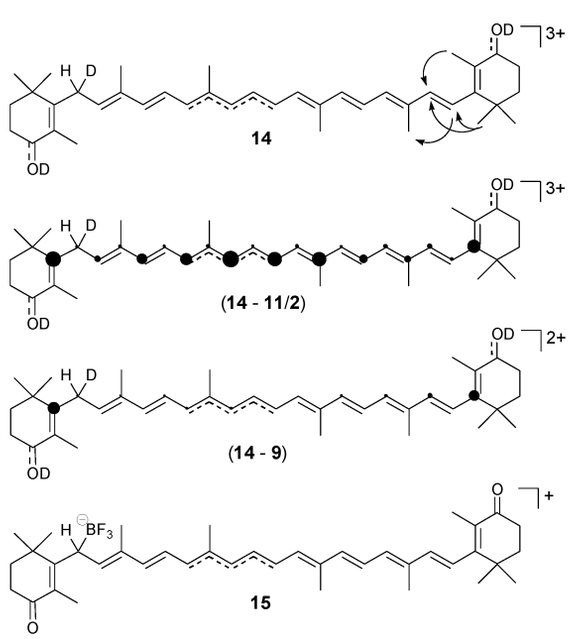

Scheme 5

The calculated change in chemical shift ($\Delta\delta_C$) between **14** and the neutral model **11/2** is given in Table 4. The charge distribution is depicted in Scheme 5. The charge on the protonated carbonyl groups is considered below.

Table 4 ^{1}H and ^{13}C chemical shifts (ppm) and $^{3}J_{H,H}$ and $^{1}J_{C,H}$ coupling constants (Hz) for O-4,4′, C-7 triprotonated canthaxanthin (**14**), and ^{13}C chemical shift difference (ppm) between **14** and the C-7 protonated cation **9** and the model **11/2**

	14				**(14 − 9)**	**(14 − 11/2)**
	δ_C	δ_H	$^{3}J_{H,H}$	$^{1}J_{C,H}$	$\Delta\delta_c$	$\Delta\delta_c$
1	39.4				2.9	3.0
2	33.5	2.00		132	−2.5	−3.9
3	30.5	3.19		131	−2.5	−3.8
4	211.5				5.2	12.6
5	131.5				−0.6	−0.1
6	198.4				27.2	35.2
7	34.0	3.62			2.2	3.9
8	141.8	5.93			−4.1	12.0
9	140.5				1.5	5.0
10	159.9	7.27	14.4	155	1.3	22.5
11	127.6	7.01	11.8/14.4		1.6	3.9
12	165.9	7.56	11.8	157	3.3	26.6
13	143.7				0.9	7.1
14	171.5	7.87	13.3	157	2.7	37.9
15	134.7	7.25	12.8/13.3	160	1.4	4.2
16/17	25.0	1.28		129	−0.8	−1.7
18	11.1	1.91		130	−0.3	−0.3
19	12.7	2.07	H-8[a]	128	0.2	−0.1
20	12.6	2.20	H-12[a]	129	0.0	−0.1
1′	38.5				1.7	2.8
2′	34.1	1.98		132	−1.9	−3.6
3′	30.0	3.14		131	−3.0	−4.3
4′	207.3				0.8	8.6
5′	128.8				−1.6	−1.1
6′	191.3				22.5	30.4
7′	129.2	6.87	15.7	155	−3.6	5.0
8′	150.2	7.06		159	8.1	9.1
9′	147.7				−4.8	12.9
10′	141.4	6.85	12.0	156	5.1	7.2
11′	141.6	7.70	12.0/14.7		−3.4	16.9
12′	142.4	6.99	14.7	158	2.6	3.1
13′	168.7				−2.1	32.1
14′	139.3	7.06		155	0.9	5.7
15′	162.3	8.18	12.8/13.0	156	1.1	31.8
16′/17′	26.9	1.33		129	−0.1	−0.8
18′	13.7	2.12	H-7′	131	−0.1	0.0
19′	13.1	2.24	H-10′[a]	129	−0.6	0.6
20′	14.9	2.46	H-14′[a]	129	−0.1	2.2
$\Sigma\Delta\delta_C$					60.2	320.0

[a] Indicates long-range coupling from methyl groups.

Deduction of the ^{13}C chemical shift difference between O-4,4′, C-7 triprotonated canthaxanthin (14) and C-7 monoprotonated canthaxanthin (9)

Selective diprotonation of canthaxanthin at O-4,4′ could not be achieved by any of the acids employed. However, the ^{13}C chemical shift difference between the trication **14** and the monocation **9** is considered a valid model for the ^{13}C chemical shift differences between the O-4,4′ diprotonated target molecule **3** and canthaxanthin (**2**). The resulting $\Delta\delta_C$ shift difference is shown in Table 4. Attention should be made to the good agreement in ^{13}C chemical shift change caused by the O-4 protonation (C-1 to C-7 moiety) and the O-4′ protonated moiety (C-8 to C-1′ moiety), both *ca*. 30 ppm.

Assuming a linear relationship between change in ^{13}C chemical shifts and charge (*cf.* the Spiesecke–Schneider relationship[26]), the distribution of the charge on the polyene of (**14** − **9**) is as illustrated by the diameter of the filled circles in Scheme 5.

The relationship is not valid, however, when change in hybridisation occurs. Contrary to the ^{13}C downfield shift of *ca*. 250 ppm[19–21,24] upon the formation of a carotenoid monocation, it is known that by protonation of non-conjugated carbonyl groups, the ^{17}O NMR signal is shifted about 260 ppm upfield.[27,28] The reason for this upfield shift is that in ^{17}O NMR, the hybridisation is more important for the chemical shift than the charge on oxygen. For the protonation of acetone, a reduction in the π bond order of 40% has been found.[27] The determination of the charge on oxygen atoms by ^{17}O NMR is therefore not straightforward.

The implication of this consideration for the charge distribution of the protonated conjugated carbonyl groups in **14** is therefore that the charge on C-4/4′ cannot be directly estimated from the change in ^{13}C chemical shift, which would indicate that there is almost no charge ($\Delta\delta_{C\text{-}4}$ = 0.8 ppm, $\Delta\delta_{C\text{-}4'}$ = 5.2 ppm, Table 4) on the carbonyl carbons.

An estimate for the carbonyl groups in (**14** − **9**) can be made, however, by assuming a 40% decrease in the π bond order upon protonation of O-4,4′ also for canthaxanthin (**2**), and by using the δ_C value for C-4 of **12** and **13** as the value expected for a C(sp^2)–O(sp^3) carbon. This gives an expected chemical shift for C-4′ of 184.7 ppm (151.9 ppm *40% + 206.5 ppm *60%), and a $\Delta\delta_C$ of 22.6 ppm, and for C-4 an expected shift of 184.5 ppm (151.9 ppm *40% + 206.3 ppm*60%), and $\Delta\delta_C$ 27.0 ppm. The accuracy of this estimate is not readily assessed, but it seems likely that it is rather underestimating than overestimating the charge located at C-4.

Since the ^{13}C chemical shift difference for O-4,4′, C-7 triprotonated canthaxanthin (**14**) relative to C-7 monoprotonated canthaxanthin (**9**) has been deduced to be *ca*. 30 ppm downfield shift per positive charge, excluding the carbonyl carbons treated separately above, it may be inferred that around 86% of the positive charge is located at the protonated carbonyl moiety,

and that the remaining charge (14%) is located on the polyene system.

Moreover, charge repulsion from the positive charge at O-4′ may also force the centrally located charge away from that end of the molecule (to the left on structure **14**, Scheme 5), causing the higher downfield shifted C-8 to C-15 region of the trication **14** compared to the monocation **9**, Table 4.

Treatment of canthaxanthin (2) with BF_3–etherates

The reactions of canthaxanthin (**2**) with Brønsted acids were supplemented with its reaction with the Lewis acid BF_3–etherate[19] in CH_2Cl_2 at −20 °C, which gave an initial product showing λ_{max} 841 nm. The reaction progressed to a second product with λ_{max} 778 nm. NMR studies at −5 °C resulted in the structural assignment for this cation (**15**) with BF_3 addition at C-7, Scheme 5. ^{1}H chemical shifts for **15** are given in the Experimental section. Hydrolysis of **15** provided *cis*-isomerised canthaxanthin (**2**).

Treatment of astaxanthin (1) with acids

VIS/NIR spectra observed when treating astaxanthin (**1**) with CF_3COOH were recorded, showing two absorption maxima at λ_{max} 508 and 872 nm (−15 °C in CH_2Cl_2), in accordance with the canthaxanthin (**2**) experiments. NMR experiments of astaxanthin (**1**) treated with BF_3–etherate failed due to the formation of black precipitate.

Discussion

Treatment of canthaxanthin (2) with selected Lewis (BF_3) and Brønsted (CF_3COOH, CF_3SO_3H) acids

In contrast to the reaction of β,β-carotene (**4**) with BF_3–etherates, where the dication **5** was readily formed and an intermediate BF_3 adduct was caught only in an MS experiment,[20] canthaxanthin (**2**) provided the monocation **15** with BF_3 added to C-7 when treated with BF_3–etherate.

The above mentioned λ_{max} at 841 nm observed during the formation of **15** may be caused by an intermediary cation radical, supported by the broadening of the initial NMR signals.[20]

Protonation at C-7 was likewise observed for treatment of **2** with Brønsted acid (CF_3COOH) providing the cation **9** in a 2 : 3 mixture with the C-5 protonated **10**.

The formation of the products **12** and **13** by preferred enolisation of O-4 monoprotonated canthaxanthin, Scheme 4, is considered plausible. The reaction of canthaxanthin (**2**) with CF_3COOH has previously been studied without detailed product analysis.[22,29]

A stronger Brønsted acid (CF_3SO_3H) was required for diprotonation at O-4,4′, which only occurred together with C-7 protonation providing the trication **14**.

NIR absorption of canthaxanthin (**2**) protonated with CF_3COOH showed high stability of the product mixture with less than 4% decrease in λ_{max} 871 nm during 24 h at −20 °C. By NMR experiments at −15 °C during more than 12 h no signs of decay were observed for any of the protonated products **9**, **10**, **12** or **13**. Thus the stability was higher than for the cations **5**, **7** and **8**.[20,21] However, the lower stability of the trication **14** and the monocation **15**, formed by addition of BF_3 was comparable to that of the cations **6**, **7** and **8**.[20,21]

The configuration/conformation of the cyclic end groups relative to the polyene chain needs particular attention. For the neutral 4-keto-β-end groups in **9** and **10**, no rotation of the C-6,7 bond was noted, which is also the case in neutral canthaxanthin (**2**) according to X-ray[30] and NMR data. For the enolised end group, both 6-*cis* and 6-*trans* isomers (**12** and **13**) were documented by ROESY data. The observation that the protonated canthaxanthin end group of the trication **14** has free rotation, as shown by the ROESY data visualised in Scheme 5, and only one set of ^{1}H chemical shifts for Me-16/17/18, is important for the conformation of astaxanthin (**1**) in crustacyanin, *vide infra*.

The bathochromic shift from 484 nm to 503 nm when treating canthaxanthin (**2**) in CH_2Cl_2 with a low concentration of CF_3COOH could not be ascribed to O-4,4′ protonation by NMR at −15 °C. The observed signal broadening of all resonances associated with the polyene chain must be a consequence of weak hydrogen bonding/interactions in the intermediate exchange domain between the acid and **2**, leaving the aliphatic region of the end group relatively unaltered, and therefore, observable.

Comparison of experimental results with previous AM1 calculations

Results have been published of AM1 (Austin Model 1) calculations for protonated canthaxanthins,[22] including the C-7 protonated (**9**), C-5 protonated (**10**) and enolised O-4 protonated (**12**) canthaxanthins studied here.

The previously calculated favoured protonation of the keto groups[31] was later reconsidered in favour of in-chain protonation.[22] The lowest ΔH_0 for the protonation of canthaxanthin (**2**) was obtained for C-7. Calculated relative heats of formation for the carbocations ($\Delta\Delta H_0$) of protonated canthaxanthins were C-7 < C-5 < C-11 < C-9 < O-4.[22] Our results suggest protonation at C-5 > C-7, whereas no conclusion can be made as to the ease of O-protonation. No protonation was observed at C-9 and C-11.

The AM1 calculated charge distribution for C-5 protonated canthaxanthin (**10**) predicted the highest positive charge at C-9, C-11, C-13, *etc*., whereas our experimental results favour the highest positive charge at C-10, C-12, C-14, *etc*. Calculated bond lengths are more according to the experimental data. AM1 calculations favour conjugated double bonds in **10** from the left side including the C-12,13 bond and from the right side of the molecule until the C-11′,12′ bond and with bond inversion in the centre of the molecule. Experimental data reveal bond inversion between C-10 and C-15′ according to the NMR coupling pattern, thus displaced relative to the calculations.

Also for C-7 protonated canthaxanthin (**9**) the AM1 calculations failed to predict the charge distribution. As for the C-5 protonated analogue (**10**) the highest positive charge was claimed at C-9, C-11, C-13, *etc*. whereas the NMR data show delocalisation of the charge mainly to C-10, C-12, C-14, *etc*. The calculated bond lengths of **10** are in better agreement with the NMR coupling constants. The experimentally determined region for double bond inversion was between C-12 and C-15′, whereas the calculated region was between C-14 and C-13′.

For the enolic O-4 protonated canthaxanthin (**12**), calculated and experimental data are in agreement concerning the carbon atoms (C-4, C-6, C-8, *etc*.) available for delocalisation of the positive charge. However, NMR data reveal a preference for delocalisation of the charge in the central part of the molecule, which is not obvious from the calculations.

It is evident that experimental studies of carotenoid cations by NMR are essential for detailed structure elucidation including bond type/region for bond inversion, charge distribution and stereochemistry of the polyene chain and the conformation/configuration of end groups relative to the polyene chain.

VIS/NIR spectra of carotenoid cations and carotenoproteins

Charge delocalisation on the polyene chain of carotenoid cations results in a lower transition energy, leading to absorption in the NIR region. The λ_{max} of the carotenoid mono-, di- and trications compiled in Table 5 are in the NIR region between 690 and 1030 nm. The position of λ_{max} is influenced by several factors; the length of the polyene chain available for electron delocalisation,[19–21] size of the charge, counterions,[19,32] solvents and temperature.[21]

Table 5 Observed and calculated λ_{max} (nm) of carotenoid mono-, di- and trications, and of carotenoproteins

Compounds	λ_{max}/nm
Isocryptoxanthin monocation (**7**, **8**)[21]	1028[a]
β,β-Carotene dication (**5**)[19,20]	920[b]
Monoprotonated canthaxanthin (**9**, **10**, **12**, **13**)	871[a]
C-7, O-4,4′-triprotonated canthaxanthin (**14**)	692[a]
Canthaxanthin + 13 mM CF_3COOH	503[a]
O-4,4′-diprotonated astaxanthin[8]	609[c], 644[c]
Asteriarubin[3]	540[d]
Alloporin[4]	545[d]
Linckiacyanin[5]	612[d]
α-Crustacyanin[2]	630[d]
β-Crustacyanin[6]	585[d]

[a] CH_2Cl_2, −15 °C; [b] $CHCl_3$, −20 °C; [c] Calc., rt; [d] Aqueous buffer, rt.

Table 6 Change in ^{13}C chemical shift, δ_C (ppm), of ^{13}C labelled positions in α-crustacyanin compared to astaxanthin (**1**)[8]

^{13}C labelled C	δ_C, **1**	δ_C, Crustacyanin	$\Delta\delta_C$
4/4′	201, 0	203, 4	2,4
12/12′	140, 2	145, 1/147, 2	4,9/ 7,0
13/13′	137, 1	135, 2	−1,9
14/14′	134, 1	138, 0/140, 9	3,9/ 6,8
15/15′	130, 1	129, 5	−0, 6
20/20′	11, 5	11, 1	−0, 4

The bathochromic shift from 485 nm to 503 nm when treating canthaxanthin (**2**) in CH_2Cl_2 with low concentrations of CF_3COOH at −15 °C could not be associated with O-4,4′ protonation by NMR at −15 °C or −70 °C. Other interactions, such as hydrogen bonding, are considered responsible for the bathochromic shift observed. No colour shift was observed using CH_3COOH.

An experimental electronic absorption spectrum of O-4,4′ diprotonated canthaxanthin (**3**) is not available, but it has been calculated for astaxanthin (**1**), with the same chromophore, to 609 nm (AM1) and 644 nm (PM3 parametrisation),[8] which is within the same region as is observed for carotenoproteins with **1** as a prosthetic group, Table 5. In addition to **1**, asteriarubin has 7,8-didehydro- and 7,8,7′,8′-tetradehydro-astaxanthin as prosthetic groups.[3]

The restricted delocalisation of the positive charge to the polyene chain established for O-4,4′ diprotonated canthaxanthin (**3**) in the present work is compatible with the shorter wavelength spectral region of the carotenoproteins than of charge delocalised carotenoid carbocations.[19–21] The different λ_{max} of the various purified carotenoproteins, Table 5, points to a different degree of protonation of astaxanthin (**1**) in the carotenoproteins considered, which by NIR data appear to fall into two categories, Fig. 1.

O-4,4′-Diprotonated canthaxanthin (3) as a model for blue carotenoproteins

Synthetic astaxanthins (**1**) with ^{13}C labelling in the C-4, 12, 13, 14, 15, 20, 4′, 12′, 13′, 14′, 15′ and 20′ positions have been used in recombination studies with the apoprotein of α-crustacyanin.[8] The ^{13}C chemical shift differences between astaxanthin (**1**) bound in crustacyanin, obtained by MAS NMR, and free **1** are cited in Table 6.

In order to create a simple model for astaxanthin (**1**) in crustacyanin, we aimed at protonation of the carbonyl oxygen atoms of canthaxanthin (**2**) by Brønsted acids. Despite not being able to selectively protonate the two carbonyl oxygen atoms, a good model for the charge distribution of O-4,4′-diprotonated canthaxanthin (**3**), and thus also O-4,4′-diprotonated astaxanthin, has been elucidated.

The symmetrical model for **3** has been created using the difference in carbon chemical shifts of C-1′ to C-20′ between the trication **14** and the monocation **9**, Table 4, and correcting the charge on the polyene chain for the part of the charge delocalised to the C-8 to C-15 region.

Expected change in ^{13}C chemical shifts for the carbon atoms in the polyene chain upon O-4,4′ diprotonation of canthaxanthin (**2**) is shown in Fig. 4.

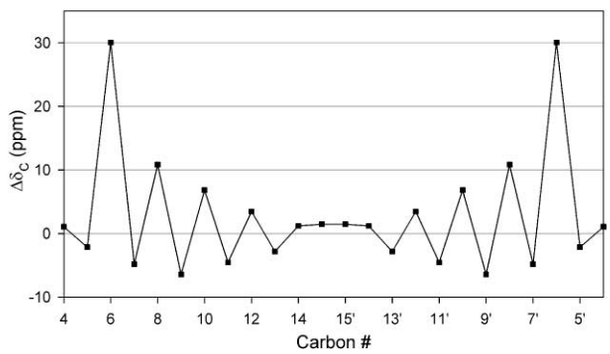

Fig. 4 Change in ^{13}C chemical shift, $\Delta\delta_C$ (ppm), of the carbon atoms in the polyene chain for O-4,4′ diprotonated canthaxanthin (**3** − **2**), based on the corrected (**14** − **9**) half model.

Scheme 6 shows the distribution of the charge in the polyene chain predicted for O-4,4′ diprotonated canthaxanthin (**3**), assuming a linear relationship between charge and change in ^{13}C chemical shift. Also shown is the estimated positive charge on the carbonyl moieties (protons, oxygen and C-4/4′ jointly). The area of the blue circles indicate lower electron density and of the red circles higher electron density than in neutral canthaxanthin (**2**), revealing C-6 ⩾ C-8 > C-10 > C-12 > C-14 ~ C-15. Interestingly, the positive charge seems to follow an exponential decrease from C-6/6′ towards the centre of the molecule. Scheme 6 also visualises the contribution of each charged structure by resonance convention.

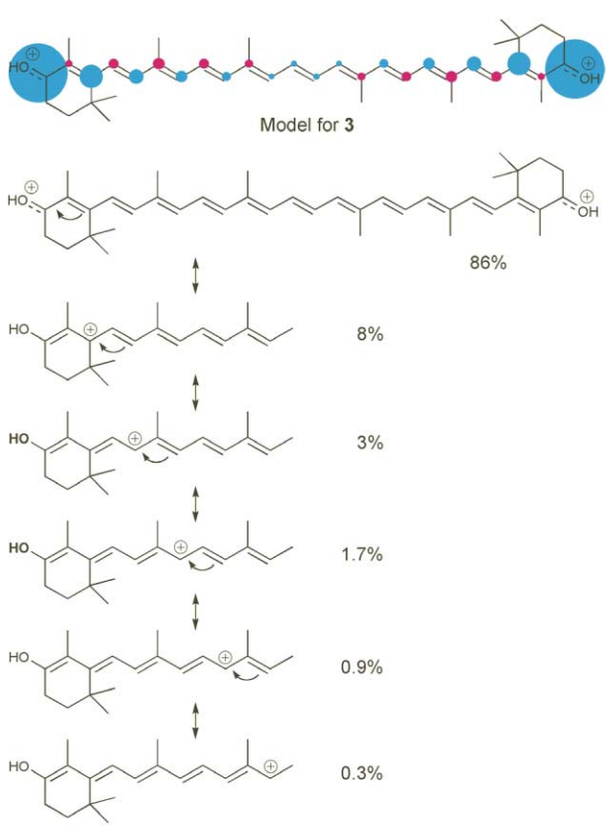

Scheme 6

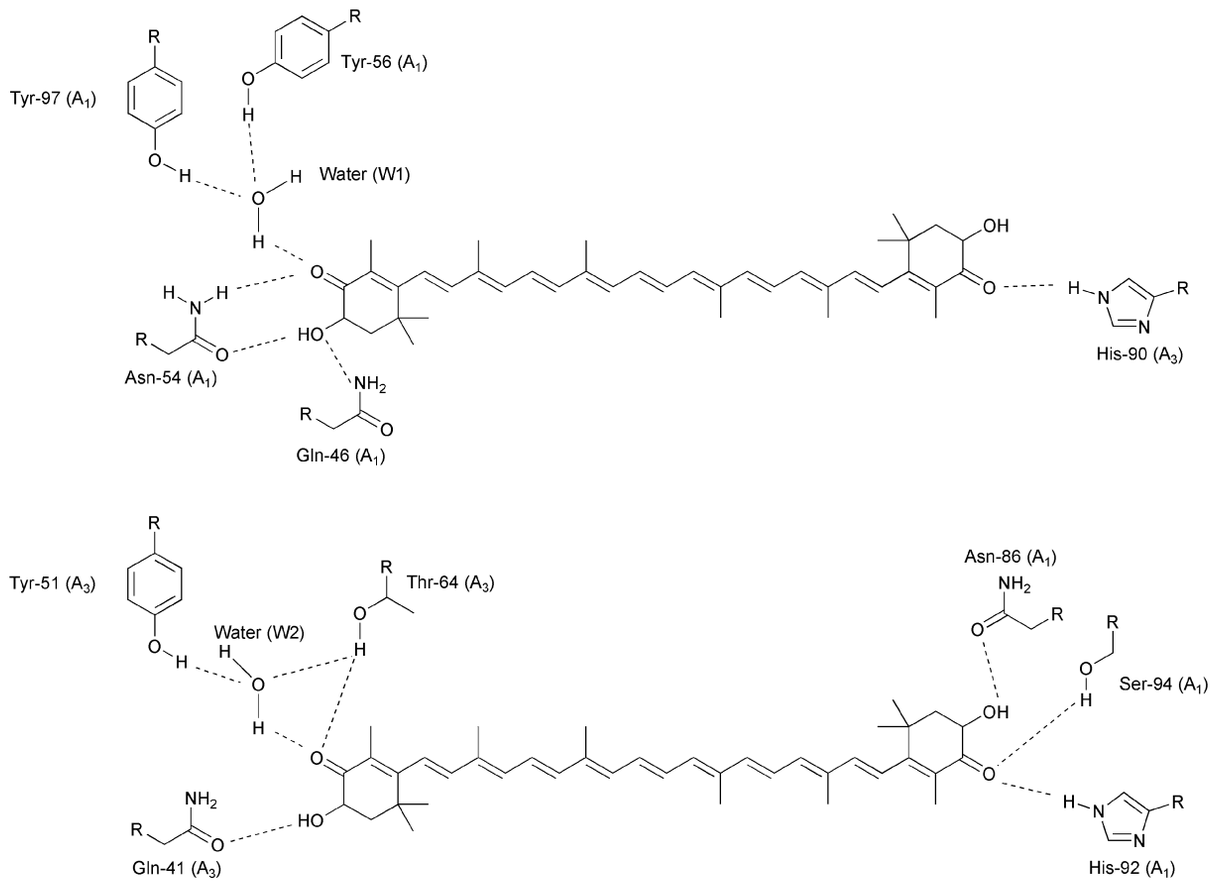

Scheme 7

The change in ^{13}C chemical shifts predicted by the model for $\Delta\delta_C$ (**3**-**2**), which is derived from ^{13}C data of the trication **14** and the monocation **9**, may be expected to show somewhat lower values in the central part of the molecule. This is due to repulsion from the third positive charge in the trication **14**, which will be centrally located as in the monocation **9**.

Nevertheless our model is in reasonable agreement with published values for α-crustacyanin, Table 6, even in the central region of the astaxanthin molecule, where the model would be expected to be less accurate due to the extra charge of the trication from which the model was derived.

A similar trend (Fig. 4) in $\Delta\delta_C$ values for astaxanthin (**1**) in α-crustacyanin is expected provided O-4,4′-diprotonation of astaxanthin (**1**) is important in α-crustacyanin.

With reference to recent high resolution X-ray data for β-crustacyanin, where the two astaxanthin molecules are located in different structural surroundings,[7,9] it is considered unlikely that full protonation of both keto groups in astaxanthin (**1**) is the case in crustacyanin and other carotenoproteins. Strong and different hydrogen bonding by adjacent water and amino acid residues are considered more likely to be responsible for the positive charge on oxygen. A simplified picture, modified from the X-ray data,[7] is shown in Scheme 7.

A notable feature of the X-ray structures[7,9] is that astaxanthin (**1**) in β-crustacyanin occurs with rotated (s-*trans*) C-6,7 and C-6′,7′ single bonds, resulting in a maximum length of the polyene chain, *cf*. **3**, Scheme 1 and Scheme 7. In this context our NMR data for the trication **14** with one O-4′ protonated end group are important by demonstrating free rotation of the C-6′,7′ single bond in the positively charged end group. Neutral astaxanthin (**1**) occurs with the opposite s-*cis* conformation of the C-6,7 single bond.

It should be pointed out that our model for fully protonated canthaxanthin (**3**) represents an extreme with complete diprotonation, case *a*) Scheme 8, whereas hydrogen bonding to one (case *b*) or two (case *c*) water, phenolic hydroxyl or amino acid >NH moieties will result in a partial positive charge on O-4,4′, with the same possibility for delocalisation of the partial charge to the polyene chain. The MAS NMR data for α-crustacyanin-bound astaxanthin, Table 6, indicate a different bonding to the keto groups.[8] Moreover, VIS-NIR data for other carotenoproteins (Table 5, Fig. 1) suggest variation in the size of positive charge on the prostethic groups (astaxanthin) caused by different degrees of hydrogen bonding.

Conclusion

A model has been developed showing the distribution of the positive charge on O-4,4′ diprotonated canthaxanthin. Approximately 86% of the charge is located on the protonated carbonyl groups and the remaining positive charge is delocalised to the polyene chain, C-6/6′ (8%) ⩾ C-8/8′ (3%) > C-10/10′ (1.7%) > C-12/12′ (0.9%) > C-14/14′ (0.3%). The charge distribution based on $\Delta\delta_C$ values (ppm) for O-4,4′ diprotonated canthaxanthin relative to canthaxanthin was determined experimentally.

The model is useful for evaluating the degree of protonation at O-4,4′ in astaxanthin bound in α-crustacyanin and other carotenoproteins, which exhibit remarkable bathochromic shifts of the electronic spectrum, and rationalises the rotation of the C-6,7/6′,7′ bonds in astaxanthin bound in crustacyanin.

The model is based on the preparation and structure determination by NIR and NMR spectroscopy of several protonated canthaxanthins, in particular the O-4,4′, C-7 triprotonated trication and the C-7 protonated monocation.

Comparison with previous AM1 calculations shows that experimental studies by NMR are essential for detailed structure elucidation of delocalised carotenoid cations, including bond type and region for bond inversion, charge distribution, stereochemistry of the polyene chain and conformation/configuration of the end groups relative to the polyene chain. In the

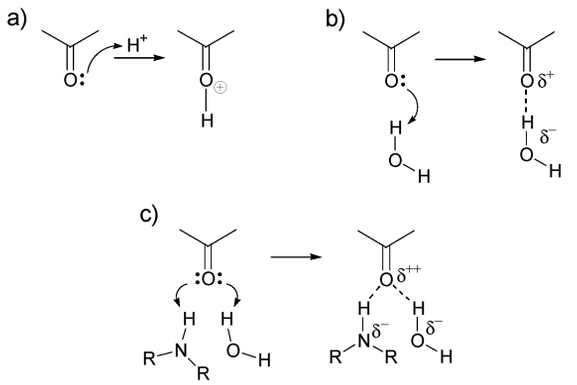

Scheme 8

present work, detailed structure elucidation has been performed with mixtures of up to four carotenoid cations.

Experimental

Materials

Synthetic astaxanthin (**1**) and canthaxanthin (**2**) were obtained from Hoffmann-La Roche, Basel. Commercially available CF_3COOH from Merck and CF_3COOD from i) Sigma and ii) Acros were used. CF_3SO_3H and CF_3SO_3D were supplied from Aldrich. Previously unopened ampoules were used in each experiment. Water content was not investigated. BF_3–diethyl etherate (BF_3–dee), BF_3–dimethyl etherate (BF_3–dme), CD_2Cl_2 and $CDCl_3$ were obtained from Acros.

General methods

Reactions and manipulations were carried out under a nitrogen atmosphere. Visible light (VIS) and near infrared (NIR) spectra were recorded on a Varian Cary 50 UV-VIS spectrophotometer (190–1100 nm). The ^{1}H NMR spectrum of neutral canthaxanthin (**2**) was recorded on a Bruker Avance DPX 400 instrument, using a 5 mm QNP probe. NMR spectra of charged canthaxanthins were obtained on a Bruker Avance DRX 500 instrument, using a 5 mm inverse probe (TXI). CD_2Cl_2 and $CDCl_3$ were used as solvents. Chemical shifts are cited relative to TMS with calibration against $CHDCl_2$ at 5.32 ppm and 53.8 ppm for ^{1}H and ^{13}C respectively, or with calibration against $CHCl_3$ at 7.27 ppm (7.37 ppm [19,20] in solutions with BF_3) for ^{1}H.

HPLC was carried out on a Hewlett Packard Series 1050 instrument equipped with a diode array detector. Detection wavelengths were set at 420, 450 and 480 nm. VIS spectra of the carotenoid components were recorded on-line during chromatography using a HPLC Technology Techsphere 5 silica column, 250 × 4.6 mm. Mobile phase: 0 min: hexane (1.5 ml min^{-1}), 30 min: hexane–acetone (85 : 15 v/v, 1.5 ml min^{-1}). Identification of *cis*-isomers of **2** was based on *cis*-peak intensity [33] A_B/A_{II}.[34]

Treatment of canthaxanthin (2) with CF_3COOH

Canthaxanthin (2). HPLC 96% all-*trans* (R_T = 16.1 min, λ_{max}/nm 467), 0.8% 13-*cis* (R_T = 17.0 min), 0.7% 9-*cis* (R_T = 17.5 min), other *ca*. 2%; λ_{max} ($CHCl_3$)/nm 484; λ_{max} (CH_2Cl_2)/nm 484 at −15 °C; δ_H(400 MHz, $CDCl_3$) 1.20 (12H, 16/17/16′/17′-H), 1.86 (4H, 2/2′-H), 1.88 (6H, 18/18′-H), 2.00 (6H, 19/19′-H), 2.01 (6H, 20/20′-H), 2.52 (4H, 3/3′-H), 6.22–6.42 (8H, 7/8/10/14/7′/8′/10′/14′-H), 6.44 (2H, 12/12′-H), 6.63–6.69 (4H, 11/15/11′/15′-H) were in agreement with published data for canthaxanthin.[35,36]

VIS/NIR experiments at −15 °C. Canthaxanthin (**2**, 16 μg) was dissolved in CH_2Cl_2 (3 ml) containing CF_3COOH (0.013 M) at −15 °C. The VIS/NIR-spectrum was recorded with the cuvette placed in a cuvette holder cooled by cold methanol (−15 °C) from a cryostat. λ_{max} 503 nm was measured, with <3% decay observed during 30 min. A weak absorption at λ_{max} 881 nm showed increasing intensity.

A higher concentration of acid (0.13 M) gave λ_{max} 506 nm (I) and 874 nm (II), initial absorption ratio (I : II) 2.2 : 1 and after 30 min 1 : 1. The combined intensity (I + II) showed no decay.

An experiment with approximately 1 M acid gave a single stable absorption maximum λ_{max} 871 nm, with <4% loss of intensity after storage at −20 °C for 24 h.

NMR analysis at −15 °C. Canthaxanthin (**2**, *ca.* 2 mg) was dissolved in a mixture of CD_2Cl_2 (0.75 ml) and CF_3COOD (0.10 ml), giving a black solution. The mixture was transferred to a chilled NMR tube and analysed by 500 MHz NMR at −15 °C. Duplicate experiments were performed with acids from both Acros and Sigma. In all freshly prepared mixtures broadened signals were observed initially, with sharp signals superimposed. During the acquisition periods, the intensity of the broadened signals decreased and were not observable after 10 h. The sharp signals increased in intensity during the experiments; however, no additional peaks occurred.

1D ^{1}H NMR, gs-COSY, 2D ROESY and gs-HSQC spectra were recorded as described previously.[20] An improved pulse-sequence for the gs-HMBC spectra was employed [37] and optimised for a $^nJ_{C,H}$ coupling constant of 8 Hz.

Pre-saturation was employed in the experiments with CF_3COOD from Acros to reduce the intensity of the $CDHCl_2$ signal in ^{1}H, COSY and ROESY spectra. An additional 2D *J*-resolved ^{1}H-spectrum was obtained from an experiment with CF_3COOD from Sigma.

NMR data for products **9** and **10** are presented in Table 1 and for products **12** and **13** in Table 3.

In a separate experiment, canthaxanthin (**2**, 1.5 mg) was dissolved in a mixture of CD_2Cl_2 (0.75 ml) and CF_3COOD (5 μl), giving a dark purple solution. The mixture was transferred to a chilled NMR tube and analysed by 500 MHz ^{1}H NMR experiments over the temperature range −70 °C to −20 °C. δ_H (sharp signals) 1.20 (12H, 16/17/16′/17′-H), 1.85 (4H, 2/2′-H), 2.66 (4H, 3/3′-H). In addition, two extremely broad resonances with maxima at 1.9 ppm and 6.4 ppm were observed.

Hydrolysis of canthaxanthin (2) after treatment with CF_3COOH. To canthaxanthin (**2**, 2.9 mg) in CH_2Cl_2 (5 ml) was added CF_3COOH (150 μl) at −10 °C. The solution turned dark brown–black. A cooled solution of 25% H_2O in acetone (8 ml) was added after 10 min. The pigments were transferred to hexane and the organic phase was washed with water and saturated NaCl solution, pigment recovery 74% ($E_{1\%,1cm}$ 2200), λ_{max} (hexane)/nm 465. HPLC 79% all-*trans* **2** (R_T = 17.2 min, λ_{max}/nm 467), 4% 13-*cis* **2** (R_T = 18.1 min, λ_{max}/nm 459, A_B/A_{II} 25%), 14% 9-*cis* **2** (R_T = 18.5 min, λ_{max}/nm 459), other carotenoids *ca*. 3%.

Treatment of canthaxanthin (2) with CH_3COOH

Canthaxanthin (**2**, 16 μg) was dissolved in CH_2Cl_2 (3 ml) containing CH_3COOH (0.017 M) at −15 °C. The VIS/NIR-spectrum was recorded with cooling as described above. A single stable maximum at λ_{max} 485 nm was recorded.

Treatment of canthaxanthin (2) with CF_3SO_3H

VIS/NIR experiment at −15 °C. Canthaxanthin (**2**, 16 μg) was dissolved in CH_2Cl_2 (3 ml) containing CF_3SO_3H (0.011 M) at −15 °C. The VIS/NIR-spectrum was recorded with cooling as described above. λ_{max} 692 nm was observed, with *ca*. 5% loss of intensity observed during 60 min.

NMR analysis at −20 °C. Canthaxanthin (**2**, 1.4 mg) was dissolved in a mixture of CD_2Cl_2 (0.75 ml) and CF_3SO_3D (5 μl),

transferred to a chilled NMR tube and analysed by 500 MHz NMR at −20 °C. A series of NMR experiments (1D ^{1}H NMR, gs-COSY, 2D ROESY, gs-HSQC and gs-HMBC) were performed in an analogous manner as described above.

NMR data for product **14** are presented in Table 4.

Treatment of canthaxanthin (2) with BF_3–etherates

VIS/NIR experiment at −20 °C. Canthaxanthin (**2**, *ca*. 20 μg) was dissolved in BF_3–dee (3.0 ml) at −20 °C. The VIS/NIR spectrum was recorded with cooling as described above. Initial λ_{max} at 841 nm showed increasing intensity for 1.5 h followed by rapid decay. New λ_{max} at 778 nm was prominent after 2.5 h. A further drop in intensity was observed (*ca*. 13% during 1 h).

NMR analysis at −5 °C. Canthaxanthin (**2**, *ca*. 1.5 mg) was dissolved in $CDCl_3$ (0.3 ml) and BF_3–dme (0.3 ml) added. The resulting black solution was transferred to a chilled NMR tube and analysed by 500 MHz NMR experiments at −5 °C. Presaturation was used to reduce the intensity of the methyl signal from the BF_3–dme reagent. Resonances were broadened in the freshly prepared mixtures, and although some improvement was observed during the acquisition period, poor line-widths combined with artefacts from the BF_3–dme reagent hampered the interpretation.

From 1D ^{1}H NMR and gs-COSY, the cation **15**, an analogous compound of **9** with BF_3 added in the C-7-position, was identified and chemical shifts partially assigned, based on the results for **9**.

Data for **15**: λ_{max} (BF_3–dee)/nm 780 (after NMR experiments); δ_H(500 MHz, $CDCl_3$/BF_3–dme) 1.28 (16/17-H), 1.33 (16′/17′-H), 1.88 (18-H), 1.99 (18′-H), 2.09 (19-H), 2.24 (20-H), 2.30 (19′-H), 2.52 (20′-H), 3.55 (7-H), 6.04 (8-H), 6.79 (10′-H), 6.82 (8′-H), 6.89 (7′-H), 6.98 (12′-H), 7.04 (11-H), 7.09 (14′-H), 7.26 (10/15-H), 7.52 (12-H), 7.86 (11′-H), 7.88 (14-H), 8.25 (15′-H).

Hydrolysis of canthaxanthin (2) after treatment with BF_3–dee. Canthaxanthin (**2**, 1.9 mg) was dissolved in $CDCl_3$ (1.0 ml) and cooled to −20 °C. Chilled BF_3–dee (1.0 ml) was added, whereupon the reaction mixture turned blue. A 1.0 ml aliquot from the mixture was transferred to a solution of 8 ml 25% H_2O in acetone, also cooled to −20 °C. The colour changed immediately back to red. The pigments were transferred to hexane and the organic phase was washed with water and saturated NaCl solution to give a pigment recovery of 79% ($E_{1\%,1cm}$ 2200), λ_{max} (hexane)/nm 463. HPLC 66% all-*trans* **2** (R_T = 17.0 min, λ_{max}/nm 465), 12% 13-*cis* **2** (R_T = 18.0 min, λ_{max}/nm 460, A_B/A_{II} 20%), 15% 9-*cis* **2** (R_T = 18.6 min, λ_{max}/nm 460), other carotenoids *ca*. 6%.

Treatment of astaxanthin (1) with acids

Astaxanthin (**1**, λ_{max} (CH_2Cl_2)/nm 486, 14 μg) was dissolved in CH_2Cl_2 (3 ml) containing CF_3COOH (0.13 M) at −15 °C. The VIS/NIR-spectrum was recorded with cooling as described above. Absorption maxima λ_{max} 508 nm (I) and 872 nm (II) were observed, initial absorption ratio (I : II) 1.9 : 1 and after 30 min 1.1 : 1. The combined intensity (I + II) showed only insignificant decay.

Attempted preparation and analysis by NMR of the cation generated upon treatment of astaxanthin (**1**) by BF_3–etherate, as described above, was unsuccessful due to solubility problems of astaxanthin (**1**) in $CDCl_3$ at low temperature, and formation of black precipitate in the NMR tube upon treatment with BF_3–etherate.

Acknowledgements

We thank professor Jostein Krane, Department of Chemistry, NTNU, for his interest in this work. Synthetic canthaxanthin and astaxanthin, as well as a research grant from Hoffmann-La Roche, Basel, to SLJ, is gratefully acknowledged.

References

1 P. F. Zagalsky, in *Carotenoids Vol 1A: Isolation and analysis*, ed. G. Britton, S. Liaaen-Jensen and H. Pfander, Birkhäuser, Basel, 1995, pp 287–294.
2 B. Renstroem, H. Roenneberg, G. Borch and S. Liaaen-Jensen, *Comp. Biochem. Physiol.*, 1982, **71B**, 249–252.
3 A. Elgsaeter, J. D. Tauber and S. Liaaen-Jensen, *Biochim. Biophys. Acta*, 1978, **530**, 402–411.
4 H. Ronneberg, G. Borch, D. L. Fox and S. Liaaen-Jensen, *Comp. Biochem. Physiol. B*, 1979, **62**, 309–312.
5 P. F. Zagalsky, F. Haxo, S. Hertzberg and S. Liaaen-Jensen, *Comp. Biochem. Physiol. B*, 1989, **93**, 339–353.
6 D. B. Gammack, J. H. Raper, P. F. Zagalsky and R. Quarmby, *Comp. Biochem. Physiol. B*, 1971, **40**, 295–300.
7 M. Cianci, P. J. Rizkallah, A. Olczak, J. Raftery, N. E. Chayen, P. F. Zagalsky and J. R. Helliwell, *Proc. Natl. Acad. Sci. U. S. A.*, 2002, **99**, 9795–9800.
8 R. J. Weesie, F. J. H. M. Jansen, J. C. Merlin, J. Lugtenburg, G. Britton and H. J. M. de Groot, *Biochemistry*, 1997, **36**, 7288–7296.
9 P. F. Zagalsky, *Acta Crystallogr., Sect. D: Biol. Crystallogr.*, 2003, **59**, 1529–1531.
10 G. Britton, R. J. Weesie, D. Askin, J. D. Warburton, L. Gallardo-Guerrero, F. J. Jansen, H. J. M. de Groot, J. Lugtenburg, J.-P. Cornard and J.-C. Merlin, *Pure Appl. Chem.*, 1997, **69**, 2075–2084.
11 J. Liu, N. L. Shelton and R. S. H. Liu, *Org. Lett.*, 2002, **4**, 2521–2524.
12 V. R. Salares, N. M. Young, H. J. Bernstein and P. R. Carey, *Biochim. Biophys. Acta*, 1979, **576**, 176–191.
13 A. A. C. van Wijk and J. Lugtenburg, in *Book of Abstracts, 13th Int. Carotenoid Symp*, Honolulu, 2002, pp. 16.
14 G. Britton, G. M. Armitt, S. Y. M. Lau, A. K. Patel and C. C. Shone, in *Carotenoid Chemistry & Biochemistry, Proc. 6th Int. Symp. Carotenoids*, ed. G. Britton and T.W. Goodwin, Pergamon Press, Oxford, 1982, pp. 237–251.
15 B. Durbeej and L. A. Eriksson, *Chem. Phys. Lett.*, 2003, **375**, 30–38.
16 J. A. Haugan and S. Liaaen-Jensen, *Acta Chem. Scand.*, 1994, **48**, 152–159.
17 R. J. Weesie, R. Verel, F. J. H. M. Jansen, G. Britton, J. Lugtenburg and H. J. M. de Groot, *Pure Appl. Chem.*, 1997, **69**, 2085–2090.
18 R. J. Weesie, J. C. Merlin, H. J. M. De Groot, G. Britton, J. Lugtenburg, F. J. H. M. Jansen and J. P. Cornard, *Biospectrosc.*, 1999, **5**, 358–370.
19 B. F. Lutnaes, L. Bruas, J. Krane and S. Liaaen-Jensen, *Tetrahedron Lett.*, 2002, **43**, 5149–5152.
20 B. F. Lutnaes, L. Bruås, G. Kildahl-Andersen, J. Krane and S. Liaaen-Jensen, *Org. Biomol. Chem.*, 2003, **1**, 4064–4072.
21 G. Kildahl-Andersen, B. F. Lutnaes, J. Krane and S. Liaaen-Jensen, *Org. Lett.*, 2003, **5**, 2675–2678.
22 V. V. Konovalov and L. D. Kispert, *J. Chem. Soc., Perkin Trans. 2*, 1999, **4**, 901–910.
23 P. v. R. Schleyer, D. Lenoir, P. Mison, G. Liang, G. K. S. Prakash and G. A. Olah, *J. Am. Chem. Soc.*, 1980, **102**, 683–691.
24 G. Englert, in *Carotenoids Vol 1B: Spectroscopy*, ed. G. Britton, S. Liaaen-Jensen and H. Pfander, Birkhäuser, Basel, 1995, pp 147–260.
25 G. Gao, C. C. Wei, A. S. Jeevarajan and L. D. Kispert, *J. Phys. Chem.*, 1996, **100**, 5362–5366.
26 H. Spiesecke and W. G. Schneider, *Tetrahedron Lett.*, 1961, **3**, 468–472.
27 G. A. Olah, A. L. Berrier and G. K. S. Prakash, *J. Am. Chem. Soc.*, 1982, **104**, 2373–2376.
28 G. A. Olah, A. Burrichter, G. Rasul, R. Gnann, K. O. Christe and G. K. S. Prakash, *J. Am. Chem. Soc.*, 1997, **119**, 8035–8042.
29 A. Mortensen and L. H. Skibsted, *J. Agric. Food Chem.*, 2000, **48**, 279–286.
30 J. C. J. Bart and C. H. MacGillavry, *Acta Crystallogr., Sect. B: Struct. Crystallogr. Cryst. Chem.*, 1968, **24**, 1587–1606.
31 A. S. Jeevarajan, C. C. Wei and L. D. Kispert, *J. Chem. Soc., Perkin Trans. 2*, 1994, **4**, 861–869.
32 J. A. Jeevarajan, C. C. Wei, A. S. Jeevarajan and L. D. Kispert, *J. Phys. Chem.*, 1996, **100**, 5637–5641.
33 L. Zechmeister, *Cis-trans Isomeric Carotenoids Vitamins A and Arylpolyenes*, Springer Verlag, Wien, 1962.
34 G. Britton, S. Liaaen-Jensen and H. Pfander, *Carotenoids Vol 1B: Spectroscopy*, Birkhäuser, Basel, 1995.
35 U. Schwieter, G. Englert, N. Rigassi and W. Vetter, *Pure Appl. Chem.*, 1969, **20**, 365–420.
36 G. P. Moss, *Pure Appl. Chem.*, 1976, **47**, 97–102.
37 R. Burger, C. Schorn and P. Bigler, *J. Magn. Reson.*, 2001, **148**, 88–94.